scientific reports

OPEN

A novel heterogeneous biocatalyst based on graphene oxide for synthesis of pyran derivatives

Leila Amiri-Zirtol & Soghra Khabnadideh ✉

Graphene oxide modified with tryptophan (GO-Trp) has been introduced as a new heterogeneous acid-base biocatalyst for synthesis of some pyran derivatives. GO was prepared according to the Hummer's method and tryptophan as a low-cost green amino acid is covalently bonded to the surface of GO without any organic or toxic reagents in a green way. The new catalyst was characterized by different spectroscopic methods such as Fourier transform infrared, X-ray diffraction (XRD), etc. …. The results of XRD patterns showed an increase in the distance between the GO plates in the presence of the modifying agent which specifies the presence of amino acid between the GO layers. XPS analysis also confirmed successful modification through the presence of C–N bonds in the structure of the catalyst. In addition, improvements in thermal stability and changes in the morphology of the samples were observed using thermogravimetric analysis and Field emission scanning electron microscopy analysis respectively. Evaluation of the catalyst performance in the synthesis of some benzo[*b*]pyran and pyrano[3,2-*c*] chromene derivatives showed presentable results. Seven benzo[*b*]pyran (*4a–4g*) and five pyrano[3,2-*c*] chromene (*4h–4l*) derivatives were synthesized. GO-Trp as a safe, natural and efficient catalyst, could be reused up to 5 runs for synthesis of pyran derivatives without any significant decrease in its potency. High purity of the products and desirable yields are other points that make the present work more attractive.

In recent decades, using of organocatalysts has been announced as a successful strategy for the greener synthesis of organic compounds[1,2]. These catalysts are small molecules, inexpensive, available and efficient organic molecules with sufficient stability and economic efficiency. They are widely used in chemical reactions while there is no need to metal for their activation[1,3,4]. Recently, the design and performance of organic–inorganic nanocomposite materials have been extensively established, mainly focusing on the ability to control their nanoscale structure via innovative synthetic approaches[5]. Amino acids as biocatalysts have both carboxylic acid and amino functional groups which led to the use of these natural compounds as dual action catalysts. The ability to easily recover and reuse the catalysts in organic evolution is highly desired economically and environmentally[6–8]. For this purpose, the use of backup is widely interested in the preparation of these catalysts[9,10]. Of the numerous known supports to date, natural-based compounds have received the most attention due to their alignment with green chemistry. Among these, carbon-based materials are very prominent due to their diverse structures. GO is one of these compounds which have a two-dimensional structure and a layer consisting of carbon, oxygen and hydrogen atoms. Having a large surface area, multiple functional groups and low intrinsic mass are some of the reasons for using GO as a strong heterogeneous support[11–13]. The specific structure of GO causes it to interact with a wide range of organic molecules through covalent or non-covalent bonds including hydrogen bonding, accumulation, hydrophobic relationships, electrostatic and van der Waals forces[14,15]. There are some reports about the respective effect of graphene and GO on human health. These carbon nanomaterials have a certain effect on human health, plants and animals. As these nanomaterials have been widely studied and applied, their effect and the potential future impact on aquatic environment should not be ignored and the knowledge about their fundamental toxicity is needed[16].

Tryptophan is an essential amino acid in the human body, containing NH_2, COOH groups, and also an indole moiety in its structure. Its acidic part ($-COO^-$) has pKa = 2.38 and its amine part ($-NH^+$) has pKa = 9.39. Despite its interesting structure and catalytic potential, its use as a heterogeneous organocatalyst in the synthesis of organic molecules is less common than the other amino acids. Aghapoor et al.[17] introduced tryptophan as a homogeneous catalyst for cyclo-condensation reactions. In 2019, Ghorbani et al.[18] used tryptophan and palladium to design a new metal catalyst to form a carbon–carbon bond.

Pharmaceutical Sciences Research Center, Shiraz University of Medical Sciences, Shiraz, Iran. ✉email: khabns@sums.ac.ir

1

On the other hand, currently, multi-component reactions are widely used as a successive strategy to synthesize different organic compounds particularly in the case of heterocycles[19]. Multi-component reactions are a group of chemical reactions in which primary substances react together and create a single product. These reactions have benefits such as easy method, high atom economy, reduction of waste generation and complex purification procedures[20–28]. Oxygenated heterocyclic compounds such as pyrans and chromones have been synthesized by using this method as well. These compounds have various pharmacological properties such as anti-cancer, anti-inflammatory[29–33], anti-coagulation[34], anti-anaphylactic[35] and anti-Alzheimer[36]. These are important structural units found widely in natural products[37]. So far, various catalysts[32–34,38–42] have been introduced for the synthesis of these compounds. Maleki et al.[43] introduced core–shell $Fe_3O_4@SiO_2$-creatine as a heterogeneous catalyst for synthesis of pyran derivatives. But this catalyst was synthesized via several steps which show hard and expensive process for preparation of this catalyst. However, some of the reported methods have drawbacks such as long reaction time, expensive reagents and long process for the synthesis of the catalyst[44].

Here we wish to introduce a novel heterogeneous biocatalyst using of tryptophan which is stabilized on the surface of GO sheets via a cost-effectiveness of method. Tryptophan was stabilized on the surface of GO by creating covalent bonds between amino acids and GO's functional groups. This heterogeneous catalyst was synthesized in a simple and green way in an aqueous media at room temperature that are noteworthy points. Using an easy and clean method with inexpensive and available materials are new strategies that are introduced in this study. As far as we know, there are no reports of tryptophan stabilization on GO. The synthesized catalyst was identified and investigated by FT-IR, XRD, X-ray photoelectron microscopy (XPS), Energy-dispersive X-ray (EDX), Raman, TGA and FE-SEM analysis. All results confirmed the placement of tryptophan on GO sheets. After decoration of tryptophan on GO and binding it to nitrogen, the amount of free carboxylic acid groups is increased. The new catalyst was used for synthesis of pyran derivatives by multicomponent reactions. Some benzo[*b*]pyran (*4a–4g*) and pyrano[3,2-*c*] chromene (*4h–4l*) derivatives were synthesized, at room temperature and green environments with high efficiency and easy separation. Chemical structure of the pyran compounds were confirmed by m.p., TLC and for some of them by spectroscopic methods. Good efficiency and short reaction time in the synthesis of pyran derivatives confirmed the high acidity of the catalyst in comparison to the GO.

In this study, tryptophan, as an amino acid, is immobilized on the surface of GO for the first time in an environmentally benign manner. The new composite was used as a novel bioorgano-catalyst for the synthesis of pyran compounds.

Results

In this research a new heterogeneous biocatalyst was introduced and identified. The catalyst capability for synthesis of some pyran derivatives under moderate conditions was evaluated as well. For synthesis of the catalyst, GO prepared according to the Hummers' method. Then tryptophan was decorated on the surface of GO in water at room temperature without any toxic or hazardous materials. The prepared composite showed significant and acceptable catalytic power in the synthesis of benzo[*b*]pyran and pyrano[3,2–*c*] chromene derivatives under moderate conditions. Immobilization of the amino acid on the surface of GO according to the epoxy groups on the surface was done easily without any toxic activators such as thionyl chloride. Using of GO also has an important role in the proper decoration of tryptophan due to its large surface area. The binding of this amino acid via covalent bonds causes the stability of the catalyst for reuse in the next reactions. The positive effect of tryptophan on the catalytic activity of the catalyst is apparent by comparison of the reaction efficiency in the presence of GO with GO-Trp. As the acidity of GO is not sufficient to carry out the reaction, its binding to tryptophan contributed to having more acidic character which led to act as a more powerful catalyst.

Catalyst identifications

FT-IR analysis

The FT-IR spectra of the GO, Trp, and GO-Trp were shown in Fig. 1. The FT-IR spectrum of GO showed certain groups with bands in certain areas. The GO absorption band in the region of 3337 cm^{-1} correspond to the
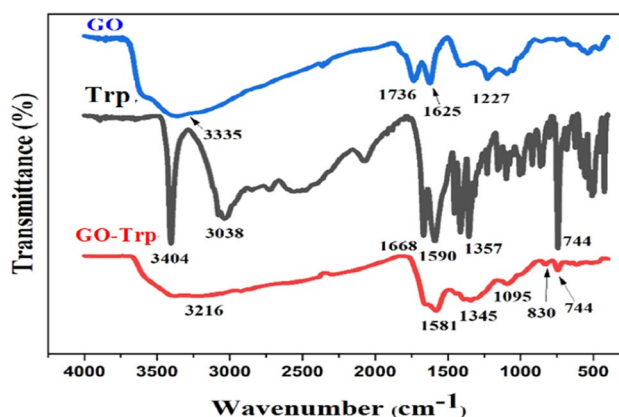
Figure 1. FTIR spectra of GO, Trp, and GO-Trp.

stretching vibrations of the OH groups on the sheet and the carboxylic acid of the GO wall. Bands in the 1736 and 1625 cm^{-1} areas are related to the stretching vibrations of the C=O and C=C groups, and bands related to the C–O and alkoxide groups were observed in the range of 1227 cm^{-1}[45]. FT-IR spectra of the amino acid showed two bands in 3404 and 3038 cm^{-1} belonging to the N–H of the indole ring and the stretching vibrations of the O–H carboxylic acid groups, respectively. The bands in the 300–2800 and 1668 areas are related to the C–H asymmetric stretching vibration and the NH_2 stretching vibration, respectively. Absorptions in the range of 400–1300 cm^{-1} are related to the other functional groups such as CNH stretching and COO^- asymmetric and symmetric stretching. By placing the amino acid on the GO sheets, certain changes such as displacement, removal and formation of some new bands were clearly visible in the related spectrum. The absorption intensity of bands at 3216 cm^{-1} for O–H and N–H stretching, at 1736 cm^{-1} for C=O, and at 1227 cm^{-1} for C–O of epoxy were decreased, which indicated GO surface changes. At 1000 to 1561 cm^{-1}, the tryptophan bands interfered with GO bands and changed the GO spectrum. The band appearing in the range 1615–1630 cm^{-1} is related to the stretching vibration of the C=C groups, and N–H, which overlaps with the band corresponding to the $-COO^-$ groups. The band appearing in 1345 cm^{-1} belonged to the bending vibration of the CH_3 groups. The resulting spectrum showed that the organic compound is located on the surface of GO.

Morphological studies
The surface of GO had wrinkles and irregularities due to the oxygen and hydroxyl groups located on the surface (Fig. 2a–c). By placing of tryptophan on the surface of GO, significant changes in the morphology of the catalyst could be observed. Changes in the GO-Trp surface indicate the modification of GO with the amino acid (Fig. 2d–f). By placing of amino acid to the surface of GO, a three-dimensional porous composite with a high surface area was created. This spongy composite may help to better interaction between the starting materials of the reaction.

XRD analysis
In the XRD pattern of GO, two peaks at 10.35° and 42.37° were observed[46]. Adding of tryptophan to the GO presented three phases in the XRD pattern including GO, rGO, and tryptophan. Peaks positions for GO are at 10.49° and 42.43°, rGO showed a broad peak at 25.07° and tryptophan has two peaks in 8.61° and 28.19°[47–53]. These results indicated that tryptophan has succeeded to some extent reduced the GO. It means the tryptophan has been able to remove some of the hydroxyl groups (–OH) of the GO. For more visibility, the quantitative phase calculation was performed on the GO-Trp sample according to the related equation from the literature (considering the dominant peak for each phase)[54]. The obtained results show ~ 37.83%, 31.49%, and 30.67% for GO, rGO, and tryptophan, respectively. Moreover, the peak position for GO shifted to a higher position after linked to the tryptophan (Fig. 3). According to the Bragg law ($n\lambda = 2d\sin\theta$, λ is X-ray wavelength, d is inter-planner spacing, and θ is the position of diffraction peak), this shift can be a sign of the lower inter-planner d-spacing for GO-Trp in comparison to the GO sample[54]. This decrease can be confirmed with d-spacing values from the XRD patterns
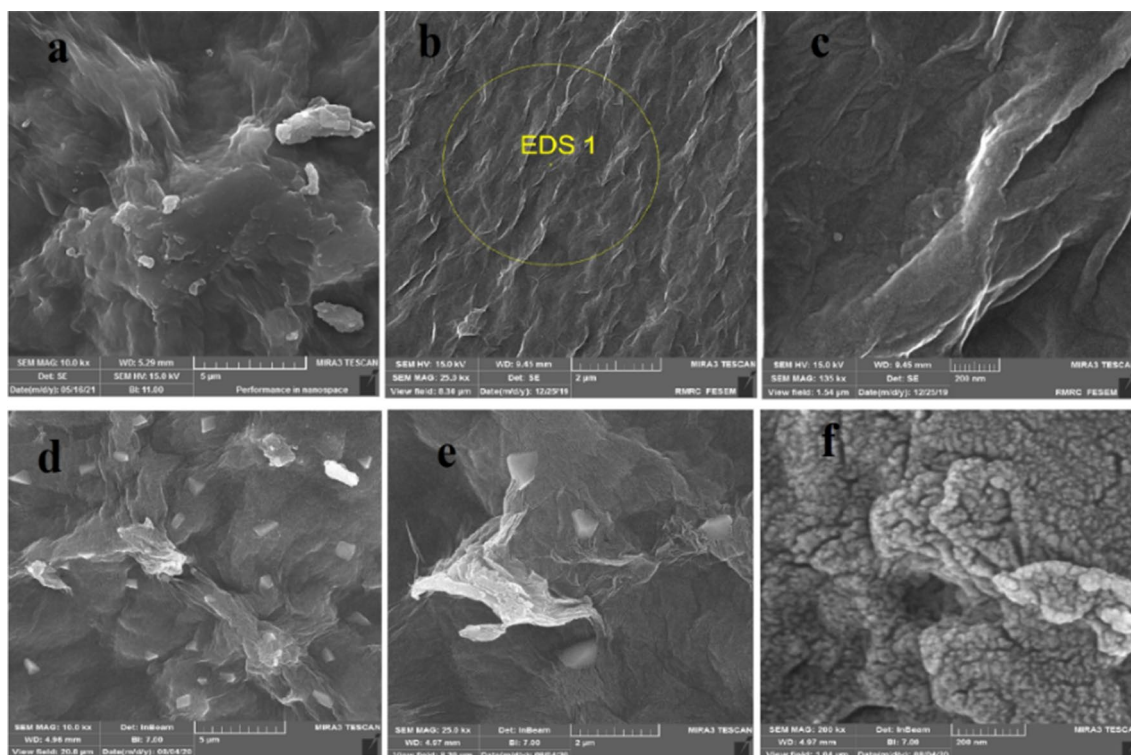
**Figure 2.** FESEM images of GO (**a**–**c**) and GO-Trp (**d**–**f**).
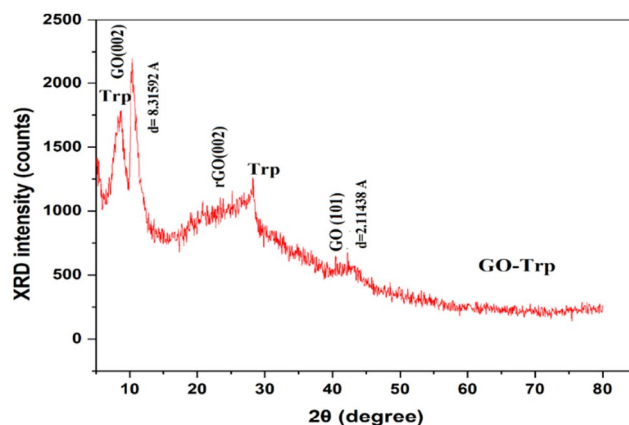
Figure 3. XRD patterns of GO-Trp.

(Fig. 3). In addition, GO peaks in the GO-Trp sample show lower intensity compared to the GO sample. This can be indicated lower crystallinity, higher disorders, and more defects by the addition of tryptophan to the GO.

XPS analysis
Figure 4 displays the XPS spectra of the GO-Trp sample. The survey scan (Fig. 4a) clearly shows the existence of the C-1s, N-1s, and O-1s peaks. Figure 4b–d presented the partial scans of the mentioned binding energy for more study. These binding energies were de-convoluted using the Gaussian function and the corresponding binding energy and their origination were labelled according to the literature[8,46,55–57]. The different peaks in the C-1s in Fig. 4b confirmed the existence of the chemical bonds related to the graphene components (GO and rGO). The obtained chemical bonds in the N-1s in Fig. 4c also confirmed the existence of the tryptophan in the catalyst. The study of the partial scan of the O-1s (Fig. 4d) beside the previous results indicated the graphene linked to tryptophan from the nitrogen side.
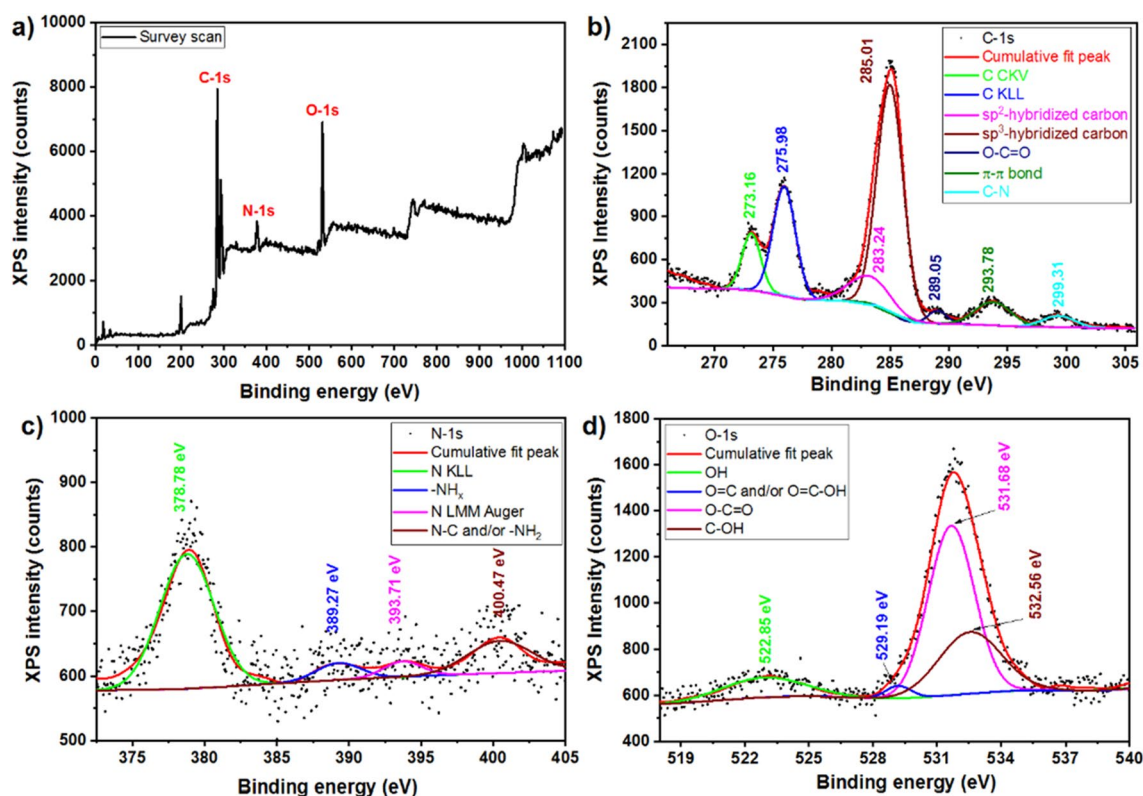
Figure 4. XPS spectra of GO-Trp, survey scan (**a**), partial scan of C-1s (**b**), N-1s (**c**), and O-1s (**d**).
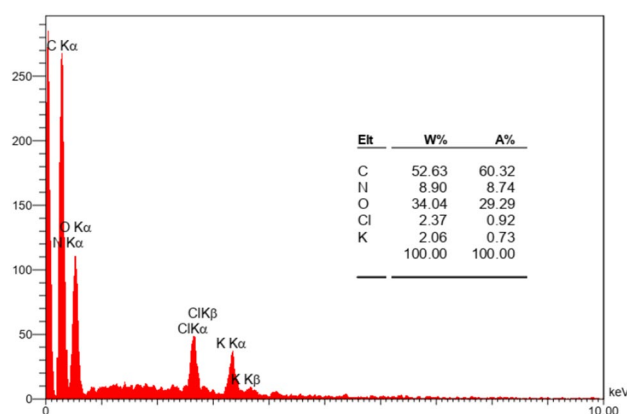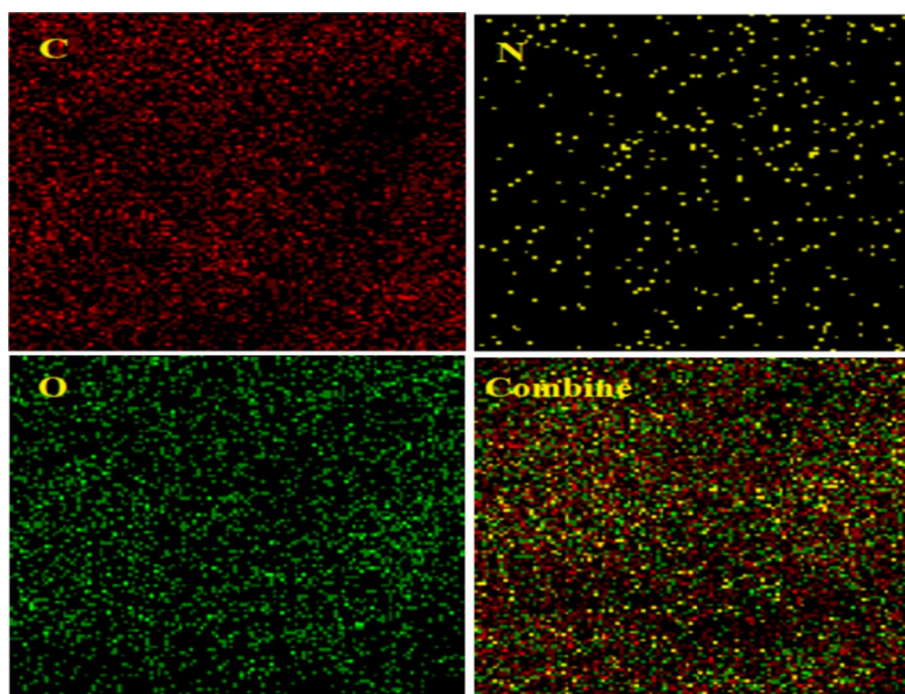
EDX analysis

In this analysis, the initial values of C, N, and O by weight percentage (%W) were shown as 50.37, 13.59, and 35.69, respectively (Fig. 5). According to this analysis, the presence of N, O, and C elements in the catalyst, confirmed the presence of the amino acid in its structure. To examine how the elements in the composite were distributed, a mapping analysis was also performed (Fig. 6). EDX-mapping also showed the presence of N in the composite, indicating the entry of tryptophan into the composite structure. These images also showed the distribution of the elements in the GO-Trp catalyst. The EDX-mapping analysis also shows a good and uniform distribution of N, C, and O elements on the surface of GO.

Raman study

Raman study is a fast and non-destructive method for investigation of the phase purity and structural features of carbon-based materials. Figure 7 represented the Raman spectra of GO and GO-Trp samples. The Raman spectra of the GO sample clearly demonstrated the carbon vibration bands belong to the GO materials[58]. In the GO-Trp Raman spectra, the vibration band of the tryptophan was also observed (~ 1051 cm^{-1})[59]. Moreover, the I_D/I_G is a proper tool for the evolution of the existence of the rGO component in the GO-Trp sample. This ratio for all samples was calculated and shown in Fig. 7. According to the literature[46], when this ratio was near unity, the reduction of the GO happened. So, the Raman results also confirmed the rGO component formation on the

Figure 5. EDX analysis of GO-Trp.

Figure 6. EDX-mapping analysis of GO-Trp.
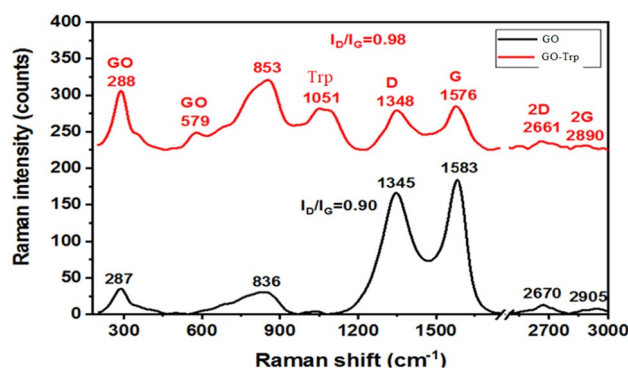
Figure 7. Raman spectra of GO and GO-Trp.

GO-Trp sample in a harmony with the XRD results. In addition, increasing the I_D/I_G ratio can be implied on more defects and disorders in agreement with the XRD results[8,60].

TGA analysis

TGA analysis can be used to determine the amount of bonded amino acids in this catalyst. At 150–600 °C, covalent bonds between amino acids and GO plates were eliminated. According to the TGA analysis of GO and GO-Trp, amino acid-functionalized GO showed desirable thermal stability (Fig. 8). In TGA analysis of GO, there are a low percent (15%) weight losses at 100 °C, which are mostly caused by moisture evaporation from the graphene oxide. Moreover, the heat treatment's elimination of GO's oxygen-containing functional groups is responsible for the main weight loss that happens in the vicinity of 200 °C. As the temperature rises, the GO experiences a thermal reduction and graphene is agglomerated into the graphite form.

In TGA analysis of GO-Trp, at 100–150 °C, the first failure occurred which is related to the removal of water. The second failure occurred at 150 °C, which is related to the removal of oxygen-containing groups. This weight loss led to the production of CO_2, CO, and water vapour[30]. The residual mass after failure was 40%. Compared to GO, amino acid-functionalized GO had less weight loss due to the reduction in the amount of oxygen-containing functional groups on the surface of graphene flakes. This weight loss was about 18% and is due to the thermal decomposition of organic groups on the GO plate (residual weight 72%). This is evidence of the successful presence of tryptophan molecules on GO plates, which due to the chemical bonds created by tryptophan increased pyrolysis resistance in comparison to GO.

Optimization of the reaction conditions

To achieve the most favourable conditions for the designed catalyst, three-component reaction of malononitrile, benzaldehyde, and daimedone for synthesis of **4a** was selected as a model reaction. Different parameters such as catalyst, solvent, temperature and amount of catalyst were evaluated. In the first step, the model reaction was tested in the presence of GO and GO-Trp in ethanol at 60 °C to confirm the catalytic properties of tryptophan. A comparison of the reaction times and yields showed the effectiveness of tryptophan in the reaction (Table 1,
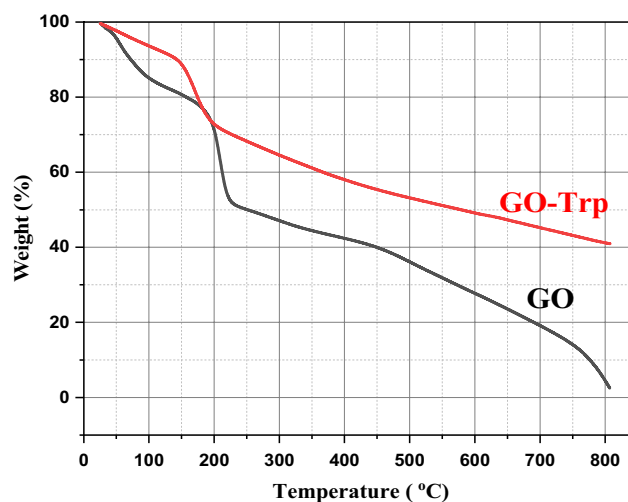
Figure 8. TGA curve of GO and GO-Trp.

Entry	Catalyst	Weight of catalyst (g)	Temp. (°C)	Solvent	Time (min)	Yield (%)
1	GO	0.04	60	EtOH	40	55
2	GO-Trp	0.04	60	EtOH	25	96
3	GO-Trp	0.04	60	Solvent-Free	20	92
4	GO-Trp	0.04	60	CH$_3$CN	65	41
5	GO-Trp	0.04	60	H$_2$O	70	80
6	GO-Trp	0.04	60	EtOH/ H$_2$O(1:1)	25	96
7	GO-Trp	0.04	r.t	EtOH/ H$_2$O(1:1)	25	96
8	**GO-Trp**	**0.03**	**r.t**	**EtOH/H$_2$O**(1:1)	**25**	**96**
9	GO-Trp	0.02	r.t	EtOH/ H$_2$O(1:1)	40	82
10	GO-Trp	0.01	r.t	EtOH/ H$_2$O (1:1)	60	70

Table 1. Optimization of the reaction conditions for synthesis of **4a**. Significant values are in bold.

rows 1–2). In the next step, the reaction was performed in different solvents and also solvent-free conditions. According to the results, the best media for the reaction was water/ethanol (1:1) (Table 1, rows 2–6). To determine the best temperature for the reaction, the model reaction was performed at room temperatures and 60 °C. As increasing the temperature had no effect on the reaction progress, the room temperature was selected due to its cost-effectiveness (Table 1, rows 6–7). Finally, to find the required amount of catalyst, the reaction was performed in four different amounts of the catalyst. In 0.03 g of catalyst, the best efficiency and the shortest time were obtained (Table 1, rows 7–10). In conclusion, the best conditions for the synthesis of the desired compounds were selected by performing the reactions in ethanol/water at room temperature with 0.03 g of the catalyst.

Catalytic activity of GO-Trp in the synthesis of pyran derivatives

After finding the best conditions some benzo[*b*]pyran (**4a–4g**) and pyrano[3,2-*c*] chromene (**4h–4l**) derivatives were synthesized under the optimized conditions (Table 2). Final products were identified by TLC and comparing their m.p. with those reported in literature. Additionally chemical structures of some compounds were checked by FT-IR, HNMR and CNMR. Their spectra are added to the supplementary file. Our results showed that the presence of electron acceptor groups on the aldehyde increases the efficiency of the reaction compared to the electron donor groups. This is due to increase the electrophilic properties of aldehyde's carbonyl groups. So, it can interact more easily with the acidic part of the catalyst and provides the conditions for a suitable reaction with nucleophilic groups. The proposed mechanism for the synthesis of the pyran derivatives is shown in Fig. 9. The synthesized nanocomposite with a layered structure and both acidic and basic moieties could progress the reaction easily. At first, the amine part of the catalyst takes a hydrogen from the malononitrile and makes it capable to attack to the carbonyl of aldehyde. In the other hand the oxygen atom of the carbonyl group interacts with the acidic part of the composite. These events causes the aldehyde carbon to become more positive. Next, the dimedone in the presence of the catalyst is converted into the enolate form. This enolate form reacted to the intermediate (I) and produce intermediate (II). Next, the removal of acidic hydrogen by the basic part of the catalyst and an intramolecular reaction lead to the production of the final compound.

Reusability of the catalyst

In order to check the reusability of the catalyst, GO-Trp was isolated from the reaction medium, washed with hot ethanol and then dried at 60 °C overnight. The dried catalyst was used in the subsequent iterations of the model reaction. The results showed that the catalyst efficiency was acceptable until 4 re-uses of the catalyst, which could be due to the complete separation of the reactant residue on the catalyst surface (Fig. 10). The covalent binding of tryptophan to the GO is a key factor in the proper reusability of the catalyst.

FT-IR spectra (Fig. 11) and XRD analysis (Fig. 12) from the catalyst before and after the reaction were compared. As can be seen, there was no discernible differences between fresh and used catalyst, proposing the stability of the catalyst.
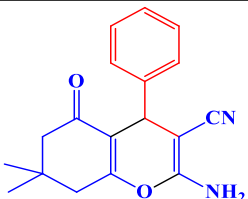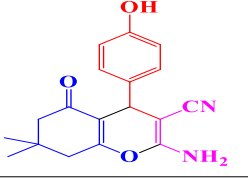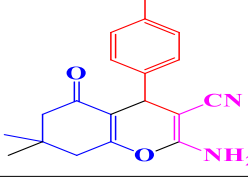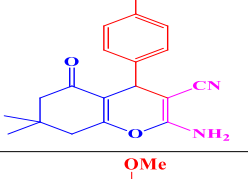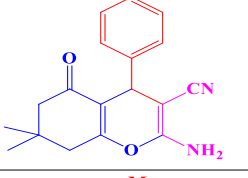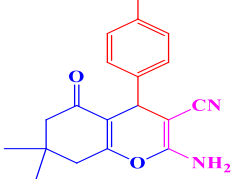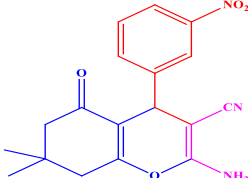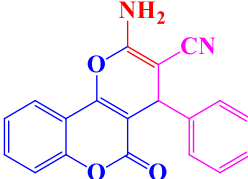
TON and TOF of the catalyst are equal to 518 mol and 20.7 min^{-1}, respectively. The high value of these two parameters indicate desirable efficiency of the catalyst.
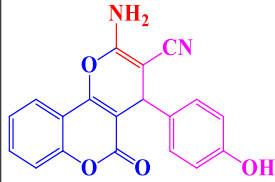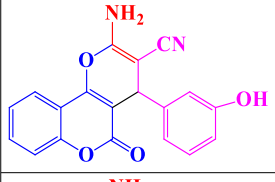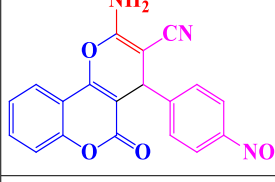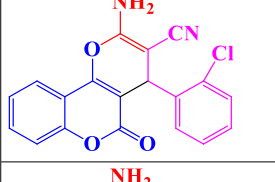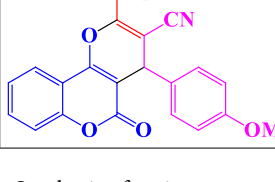
Hot filtration

In continuance of our work, hot filtration test was done on the model reaction to show the recoverability and the heterogeneity nature of GO-Trp. After 5 min from the reaction time, the catalyst was discrete by filtration from the reaction mixture and the reaction was monitored. However, no improvement in the reaction was observed in the filtrate.

Comparison of the efficiency of GO-Trp with the other reported catalysts

The efficiency of our new catalyst in the model reaction was compared with the other previously reported methods (Table 3). Easy separation and greenness of the catalyst, high yield, short reaction time and performing the reaction in room temperate are advantages of this work compared to the other previous works.

Entry	Products	Time (min)	Yield (%)	M.P. (°C) (Obs.)/(Lit.) [Ref]
4a		25	96	230–231/231–233[61]
4b		45	87	245–246/246–247[62]
4c		15	96	231–232/234–236[62]
4d		18	97	235–239/233–235[63]
4e		43	85	200–203/203–205[64]
4f		30	87	207–210/210–212[61]
4g		18	96	215–217/209–211[21]
4h		24	93	260–262/260–261[21]
Continued				

| Entry	Products	Time (min)	Yield (%)	M.P. (°C) (Obs.)/(Lit.) [Ref]
4i		32	89	245–250/261–263[21]
4j		20	91	271–273/269–270[65]
4k		20	97	250–252/255–257[65]
4l		20	91	214–218/214–216[65]
4n		27	87	250–252/244–246[17]

Table 2. Synthesis of various pyran derivatives under the optimized conditions.

Discussions

In summary, the synthesis and identification of a new and naturally catalyst was introduced as an effective and environmentally friendly catalyst to perform a stepwise reaction of pyran derivatives in ethanol–water with high efficiency. GO-Trp was synthesized easily and in a consistent manner with green chemistry in two steps. GO was first synthesized and the amino acid was then located by covalent bonding on GO plates in water at room temperature. The lack of toxic activators such as thionyl chloride, green conditions for temperate, time and solvent were the advantages of this method. Acid-base properties of the catalyst promote the progress of the desired reaction under both basic and acidic conditions. Stabilization of tryptophan molecules on the surface of graphene by covalent bonds, caused porosity, spacing of GO plates, and the formation of a GO layered structure, which improved the catalyst efficiency. The expected structure of the catalyst was verified by IR, XPS, XRD, and Raman analysis. We concluded, the catalysts consisting of both amino and acid moieties can assistance the chemical synthesis. Doing the reaction in green conditions, high efficiency and suitable purity of the products, short reaction time, cheap and non-toxic materials and reusability of the catalyst are other notable advantages of this method. Probably other amino acids can also be used instead of tryptophan to develop some more novel and green catalysts.

Methods

All chemicals were purchased from Fluka Chemical Co., Switzerland, and Merck Chemical Co., Germany, and were used without further purification. FT-IR spectra were recorded as KBr pills in the 400–4000 cm^{-1} region using Shimadzu FT-IR 8300 spectrophotometer. The characterization of the products was recorded on a Bruker AC 500 Avance DPX spectrometer at 500 MHz for ^{1}H NMR and 125 MHz for ^{13}C in the presence of TMS. The progress of the reaction was examined using thin-layer chromatography (TLC) on silica gel PolyGram SILG/UV254 plates. Melting points were measured in open capillary tubes in a Buchi melting point B-540 B. The morphology of the samples was studied through FE-SEM, MIRA3TESCAN-XMU. The phase purity of the samples was checked using the XRD analysis using Ni-FILTERED whit Cu-Ka radiation (λ = 1.5406 Å) in the 2θ range from 5° to 80°. XPS spectroscopy was performed by monochromatic Al KR (1486.6 eV) irradiation (a Perkin-Elmer PHI 6000 C/ECSA system). The elemental analysis and distribution were carried out using EDX analysis (recorded by SAMX MIRA II). Raman spectroscopy was accomplished through UniRAM Raman spectrometer
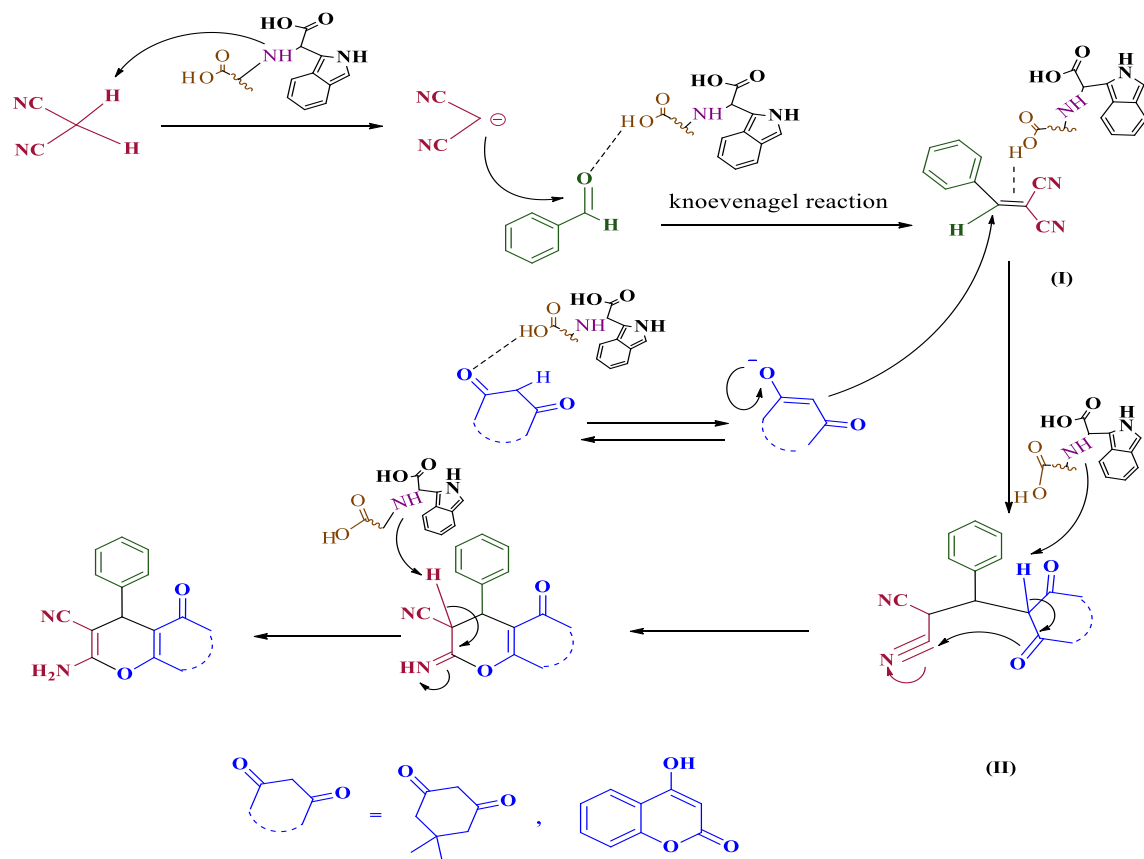
Figure 9. Schematic presentation of proposed mechanism for the synthesis of pyran derivatives in the presence of GO-Trp.
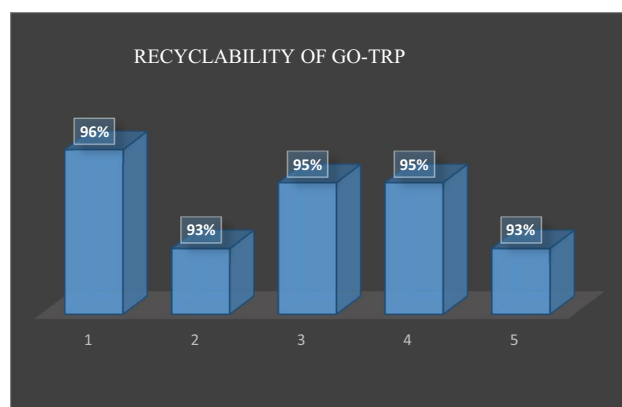

**Figure 10.** Recyclability of GO-Trp in synthesis of *4a*.

with solid-state laser source operating at a wavelength of 785 nm and 200 mW, from 250 to 3000 cm^{-1}. Thermogravimetric analysis (TGA) was performed on an STA 504 thermal analysis machine B.

Synthesis of graphene oxide modified with tryptophan (GO-Trp)
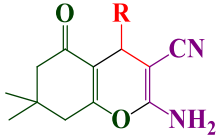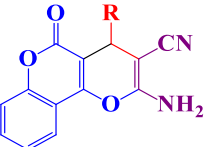
Initially, GO was prepared according to the Hummer's method[74]. Then 0.5 g of GO in 20 mL of deionized water was dispersed for half an hour. Then 0.5 g of sodium hydrate followed by 0.5 g of amino acid were added to the stirring reaction vessel. The reaction vessel was allowed to be stirred at room temperature for 24 h. Finally, the catalyst was separated by centrifugation, washed with water/ethanol and dried at 60 °C in a furnace overnight (Fig. 13).
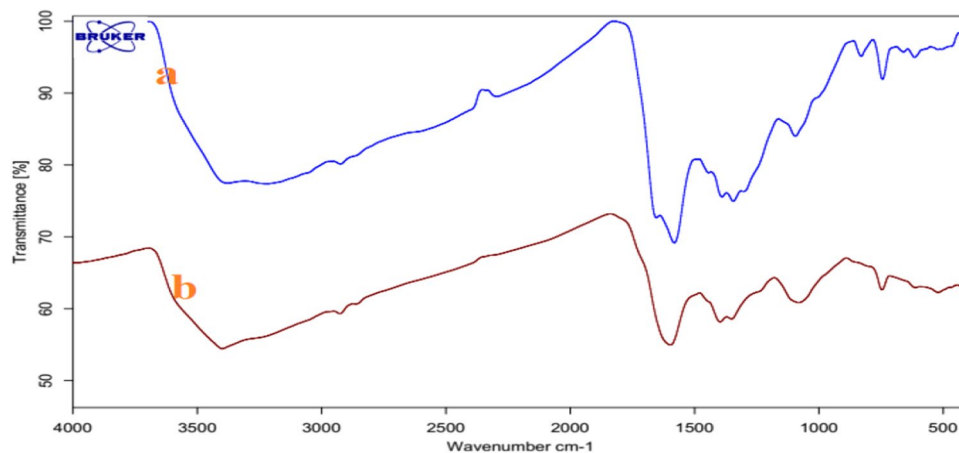
Figure 11. FTIR spectra of fresh GO-Trp (**a**) and used GO-Trp (**b**).
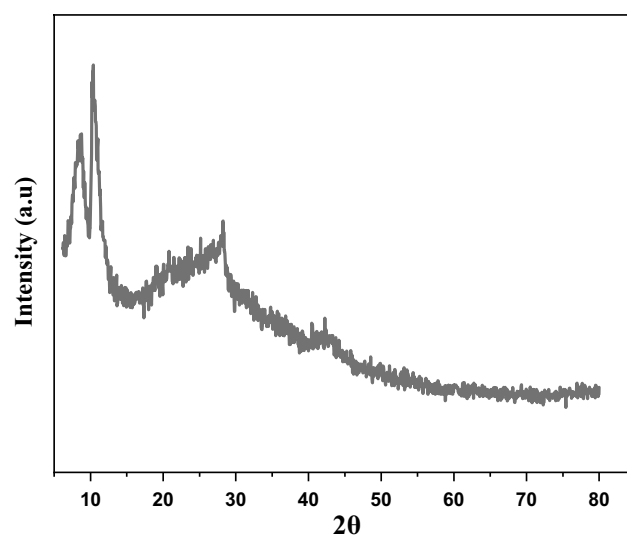
Figure 12. XRD pattern of used GO-Trp.

Product	Catalyst/Temp/Time (min)/Solvent	Yield (%)
	PC/AgNPs/reflux/35/H_2O: EtOH (1:1)	82[66]
	$BaFe_{12}O_{19}$@ IM/reflux/15/EtOH	96[67]
	$MnFe_2O_4$@$SiO_2NHPhNH_2$–PTA./80 °C/30/Solvent-free	95[64]
	GO-Arg/reflux /10/H_2O: EtOH (1:1)	93[45]
	Piperazine-GO/50 °C/15/H_2O–EtOH	95[68]
	Biocompatible Core/Shell Fe_3O_4@GA@Isinglass/reflux/15/EtOH	92[69]
	Chitosan-EDTA-Cellulose/ r.t./10/EtOH	96[70]
	GO-Trp/r.t. /25/H_2O: EtOH (1:1)	96 (This work)
	o-Benzenedisulfonimide (OBS)/120 °C/50/Solvent-free	85[64]
	PC/AgNPs/reflux/30/H_2O: EtOH (1:1)	80[66]
	PS-PTSA/80 °C/120/EtOH	94[71]
	GO-Arg/reflux/14/H_2O: EtOH (1:1)	95[45]
	[Amb]L-prolinate/reflux/20/EtOH	90[72]
	Zr@IL-Fe_3O_4 MNPs/100 °C/10/Solvent-free	96[73]
	GO-Trp/r.t./24/H_2O:EtOH (1:1)	93 (This work)

Table 3. Comparison of the efficiency of GO-Trp with other catalysts reported for synthesis of pyran derivatives.
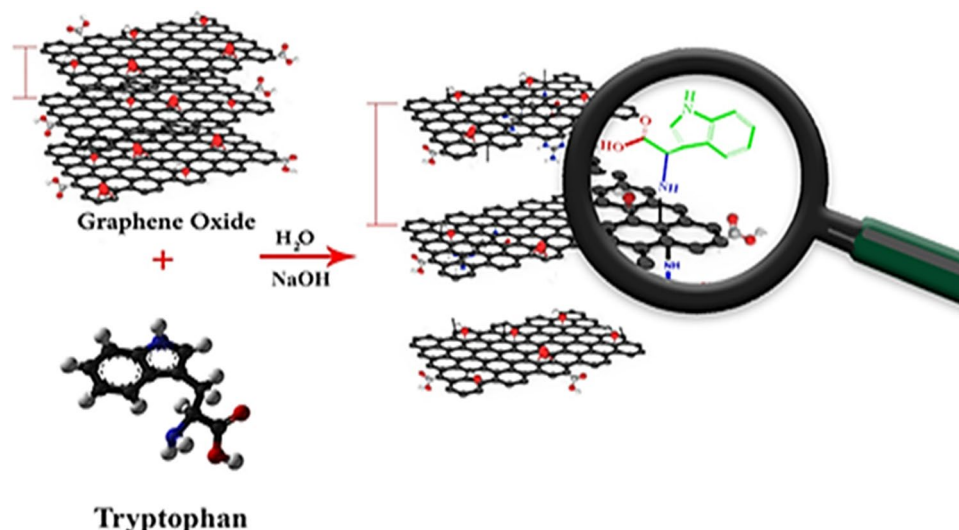
Figure 13. Schematic presentation for synthesis of the GO-Trp.
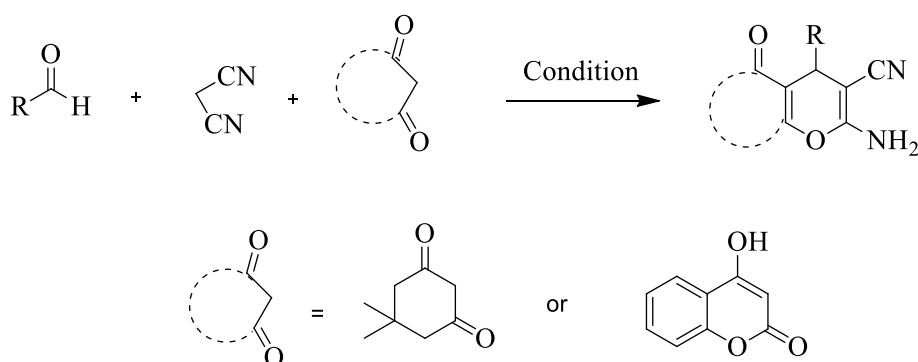
Figure 14. Schematic presentation for synthesis of the pyran derivatives using GO-Trp.

General procedure for synthesis of the pyran derivatives

After characterization of the catalyst, its activity for synthesis of benzo[*b*]pyran and pyrano[3,2-*c*] chromene derivatives were investigated. First, malononitrile (0.066 g, 1 mmol), benzaldehyde (1 mmol) and dimedone (0.140 g, 1 mmol) for benzo[*b*]pyran (**4a–4g**) and malononitrile (0.066 g, 1 mmol), benzaldehyde (1 mmol) and 4-hydroxycoumarin (0.162 g, 1 mmol) for pyrano[3,2-*c*] chromene (**4h–4l**) derivatives were poured into a 25 mL flask containing 10 mL water/ethanol. Then, 0.03 g of catalyst was added and the reaction is allowed to take place at room temperature for the required time. The progress of the reaction was checked by TLC. After the reaction completion, the catalyst was separated by centrifugation. The reaction solvent is then evaporated and the resulting precipitate is purified by recrystallization in absolute ethanol. The catalyst washed with hot ethanol and reused in the next reaction (Fig. 14).

Data availability

Data sets generated during and/or analyzed during the current study are available from the corresponding author on request.

References

1. Dangolani, S. K., Panahi, F., Nourisefat, M. & Khalafi-Nezhad, A. 4-Dialkylaminopyridine modified magnetic nanoparticles: As an efficient nano-organocatalyst for one-pot synthesis of 2-amino-4H-chromene-3-carbonitrile derivatives in water. *RSC Adv.* **6**, 92316–92324 (2016).
2. Bruera, F. A. *et al.* Laccase immobilization on nanoporous aluminum oxide for black liquor treatment. *Surf Interfaces.* **30**, 101879 (2022).

3. Cui, Y., Lee, Y. H. & Yang, J. W. Impact of carboxyl groups in graphene oxide on chemoselective alcohol oxidation with ultra-low carbocatalyst loading. *Sci. Rep.* **7**, 3146 (2017).

4. Maleki, A., Hajizadeh, Z. & Abbasi, H. Surface modification of graphene oxide by citric acid and its application as a heterogeneous nanocatalyst in organic condensation reaction. *Carbon Lett.* **27**, 42–49 (2018).

5. Maleki, A., Ravaghi, P., Aghaei, M. & Movahed, H. A novel magnetically recyclable silver-loaded cellulose-based bionanocomposite catalyst for green synthesis of tetrazolo [1, 5-a] pyrimidines. *Chem. Intermed.* **43**, 5485–5494 (2017).

6. Aghahosseini, H. & Ramazani, A. Magnetite L-proline as a reusable nano-biocatalyst for efficient synthesis of 4H-benzo [b] pyrans in water: A green protocol. *Eurasian Chem. Commun.* **2**, 410–419 (2020).

7. Nourisefat, M., Panahi, F., Nabipour, M., Heidari, S. & Khalafi-Nezhad, A. l-Cysteine-functionalized magnetic nanoparticles (LCMNP): As a magnetic reusable organocatalyst for one-pot synthesis of 9-(1H-indol-3-yl) xanthen-4-(9H)-ones. *J. Iran. Chem. Soc.* **13**, 1853–1865 (2016).

8. Mallakpour, S., Abdolmaleki, A. & Borandeh, S. Covalently functionalized graphene sheets with biocompatible natural amino acids. *Surf. Interfaces* **307**, 533–542 (2014).

9. Azad, S. & Fatameh Mirjalili, B. B. Fe$_3$O$_4$@nano-cellulose/TiCl: A bio-based and magnetically recoverable nano-catalyst for the synthesis of pyrimido[2,1-b]benzothiazole derivatives. *RSC Adv.* **6**, 96928–96934 (2016).

10. Hajipour, A. R., Boostani, E. & Mohammadsaleh, F. Proline-functionalized chitosan–palladium(ii) complex, a novel nanocatalyst for C–C bond formation in water. *RSC Adv.* **5**, 24742–24748 (2015).

11. Rezaei-Seresht, E., Bakhshi-Noroozi, M. & Maleki, B. Piperazine-grafted magnetic reduced graphene oxide (Fe$_3$O$_4$@rGO-NH) as a reusable heterogeneous catalyst for gewald three-component reaction. *Polycycl. Aromat. Compd.* **41**, 1944–1952 (2021).

12. Mallakpour, S., Abdolmaleki, A. & Karshenas, A. Graphene oxide supported copper coordinated amino acids as novel heterogeneous catalysts for epoxidation of norbornene. *Catal. Commun.* **92**, 109–113 (2017).

13. Anuradha, K. & S., Layek, S. & Pathak, D.D.,. Chitosan supported Zn(II) mixed ligand complexes as heterogeneous catalysts for one-pot synthesis of amides from ketones via Beckmann rearrangement. *J. Mol. Struct.* **1130**, 368–373 (2017).

14. Qu, K., Wu, L., Ren, J. & Qu, X. Natural DNA-modified graphene/Pd nanoparticles as highly active catalyst for formic acid electro-oxidation and for the Suzuki reaction. *ACS Appl. Mater. Interfaces* **4**, 5001–5009 (2012).

15. Eivazzadeh-Keihan, R., Radinekiyan, F., Madanchi, H., Aliabadi, H. A. M. & Maleki, A. Graphene oxide/alginate/silk fibroin composite as a novel bionanostructure with improved blood compatibility, less toxicity and enhanced mechanical properties. *Carbohydr. Polym.* **248**, 116802 (2020).

16. Liu, X. T. *et al.* Toxicity of multi-walled carbon nanotubes, graphene oxide, and reduced graphene oxide to zebrafish embryos. *Biomed. Environ. Sci.* **27**, 676–683 (2014).

17. Aghapoor, K., Mohsenzadeh, F., Darabi, H. R., Sayahi, H. & Balavar, Y. l-Tryptophan-catalyzed Paal-Knorr pyrrole cyclocondensation: An efficient, clean and recyclable organocatalyst. *Chem. Intermed.* **42**, 407–415 (2016).

18. Ghorbani-Choghamarani, A., Mohammadi, M., Hudson, R. H. E. & Tamoradi, T. Boehmite@tryptophan-Pd nanoparticles: A new catalyst for C–C bond formation. *Appl. Organomet. Chem.* **33**, e4977 (2019).

19. Maleki, A., Hajizadeh, Z. & Salehi, P. Mesoporous halloysite nanotubes modified by CuFe$_2$O$_4$ spinel ferrite nanoparticles and study of its application as a novel and efficient heterogeneous catalyst in the synthesis of pyrazolopyridine derivatives. *Sci. Rep.* **9**, 5552 (2019).

20. Adibian, F., Pourali, A. R., Maleki, B., Baghayeri, M. & Amiri, A. One-pot synthesis of dihydro-1H-indeno[1,2-b] pyridines and tetrahydrobenzo[b] pyran derivatives using a new and efficient nanocomposite catalyst based on N-butylsulfonate-functionalized MMWCNTs-D-NH$_2$. *Polyhedron* **175**, 114179 (2020).

21. Esmaeilpour, M., Javidi, J., Dehghani, F. & Nowroozi Dodeji, F. A green one-pot three-component synthesis of tetrahydrobenzo[b] pyran and 3,4-dihydropyrano[c]chromene derivatives using a Fe$_3$O$_4$@SiO$_2$–imid–PMAn magnetic nanocatalyst under ultrasonic irradiation or reflux conditions. *RSC Adv.* **5**, 26625–26633 (2015).

22. Norouzi, M., Elhamifar, D., Mirbagheri, R. & Ramazani, Z. Synthesis, characterization and catalytic application of a novel ethyl and boron sulfonic acid based bifunctional periodic mesoporous organosilica. *J. Taiwan Inst. Chem. Eng.* **89**, 234–244 (2018).

23. Maleki, B., Ashrafi, S. S. & Tayebee, R. Lewis acid free synthesis of 3, 4-dihydro-1 H-indazolo [1, 2-b] phthalazine-1, 6, 11 (2 H, 13 H)-triones promoted by 1, 1, 1, 3, 3, 3-hexafluoro-2-propanol. *RSC Adv.* **4**, 41521–41528 (2014).

24. Maleki, B., Barzegar, S., Sepehr, Z., Kermanian, M. & Tayebee, R. A novel polymeric catalyst for the one-pot synthesis of xanthene derivatives under solvent-free conditions. *J. Iran. Chem. Soc.* **9**, 757–765 (2012).

25. Atharifar, H., Keivanloo, A., Maleki, B., Baghayeri, M. & Alinezhad, H. Magnetic nanoparticle supported choline chloride-glucose (deep eutectic solvent) for the one-pot synthesis of 3, 4-disubstituted isoxazol-5 (4H)-ones. *Chem. Intermed.* **50**, 1–16 (2023).

26. Naderi, S., Sandaroos, R., Peiman, S. & Maleki, B. Novel crowned cobalt (II) complex containing an ionic liquid: A green and efficient catalyst for the one-pot synthesis of chromene and xanthene derivatives starting from benzyl alcohols. *J. Phys. Chem. Solids* **180**, 111459 (2023).

27. Maleki, A. An efficient magnetic heterogeneous nanocatalyst for the synthesis of pyrazinoporphyrazine macrocycles. *Polycycl. Aromat. Compd.* **38**, 402–409 (2018).

28. Maleki, A. & Azadegan, S. Amine-functionalized silica-supported magnetic nanoparticles: Preparation, characterization and catalytic performance in the chromene synthesis. *J. Inorg. Organomet. Polym. Mater.* **27**, 714–719 (2017).

29. Hajjami, M., Gholamian, F., Hudson, R. H. E. & Sanati, A. M. FSM-16/AEPC-SO$_3$H: Synthesis, characterization and its application for the catalytic preparation of 1,8-Dioxo-octahydroxanthene and Tetrahydrobenzo[b]pyran derivatives. *Catal. Lett.* **149**, 228–247 (2019).

30. Mhaibes, R. M., Arzehgar, Z., Mirzaei Heydari, M. & Fatolahi, L. ZnO Nanoparticles: A highly efficient and recyclable catalyst for tandem knoevenagel-michael-cyclocondensation reaction. *Asian J. Green Chem.* **7**, 1–8 (2023).

31. Baghernejad, B. & Hojjati Taromsari, S. M. Aqueous media preparation of 2-amino-4H-benzopyran derivatives using cerium oxide nanoparticles as a recyclable catalyst. *Asian J. Green Chem.* **6**, 194–202 (2022).

32. Pund, G. B., Dhumal, S. T., Hebade, M. J., Farooqui, M. & Dobhal, B. S. Meglumine catalysed green synthesis of Ethyl-6-amino-5-cyano-2-methyl-4-phenyl-4H-pyran-3-carboxylate derivatives. *J. Appl. Organomet. Chem.* **2**, 15–23 (2022).

33. Keshvari Kenari, M., Asghari, S., Maleki, B. & Mohseni, M. Preparation of nanomagnetic alginate modified by histidine as an antibacterial agent and a reusable green catalyst for the three-component synthesis of 2-amino-4 H-chromenes and tetrahydro-pyrimidines. *Chem. Intermed.* **50**, 1–20 (2023).

34. Hiremath, P. B. & Kantharaju, K. An efficient and facile synthesis of 2-Amino-4H-pyrans & tetrahydrobenzo[b]pyrans catalysed by WEMFSA at room temperature. *ChemistrySelect* **5**, 1896–1906 (2020).

35. Maleki, A., Jafari, A. A. & Yousefi, S. Green cellulose-based nanocomposite catalyst: Design and facile performance in aqueous synthesis of pyranopyrimidines and pyrazolopyranopyrimidines. *Carbohydr. Polym.* **175**, 409–416 (2017).

36. Suthar, M., Kumbhani, J. & Bhatt, K. D. Pyran heterocyclic compound as the prosperous scaffolds for biological sensor (A-review). *Oriental J. Chem.* **37**, 1280–1286 (2021).

37. Kazemi, B., Javanshir, S., Maleki, A., Safari, M. & Khavasi, H. R. An efficient synthesis of 4H-chromene, 4H-pyran, and oxepine derivatives via one-pot three-component tandem reactions. *Tetrahedron Lett.* **53**, 6977–6981 (2012).

38. Mane, V. U. & Mane, D. V. [DBN][HSO$_4$]-Promoted facile and green synthesis of 2-Amino-4Hpyrans derivatives under microwave irradiation. *J. Drug Deliv. Ther.* **11**, 89–97 (2021).

39. Yang, Z.-J. *et al.* Biocatalytic tandem multicomponent reactions for one-pot synthesis of 2-Amino-4H-Pyran library and in vitro biological evaluation. *Mol. Catal.* **491**, 110983 (2020).

40. Rohani, L., Karami, B. & Farahi, M. A green, facile, and one-pot synthesis of 2-amino-4H-pyran derivatives using tungstate sulfuric acid as a solid acid catalyst. *J. Chin. Chem. Soc.* **68**, 888–892 (2021).

41. Brahmachari, G. Chapter 1 - Green synthetic approaches for biologically relevant heterocycles: Advanced synthetic techniques—An overview. In *Green Synthetic Approaches for Biologically Relevant Heterocycles* 2nd edn (ed. Brahmachari, G.) 1–8 (Elsevier, 2021).

42. Valipour, Z., Hosseinzadeh, R., Sarrafi, Y. & Maleki, B. Natural deep eutectic solvent as a green catalyst for the one-pot synthesis of chromene and 4H-pyran derivatives. *Org. Prep. Proced. Int.* **56**, 1–13 (2023).

43. Eivazzadeh-Keihan, R., Bahrami, S., Ghafori Gorab, M., Sadat, Z. & Maleki, A. Functionalization of magnetic nanoparticles by creatine as a novel and efficient catalyst for the green synthesis of 2-amino-4H-chromene derivatives. *Sci. Rep.* **12**, 10664 (2022).

44. Maleki, A. & Hajizadeh, Z. Magnetic aluminosilicate nanoclay: A natural and efficient nanocatalyst for the green synthesis of 4 H-pyran derivatives. *Silicon* **11**, 2789–2798 (2019).

45. Khabnadideh, S., Mirzaei, E. & Amiri-Zirtol, L. L-arginine modified graphene oxide: A novel heterogeneous catalyst for synthesis of benzo[b]pyrans and pyrano[3,2-c]chromenes. *J. Mol. Struct.* **1261**, 132934 (2022).

46. Yousefi, R. & Cheraghizade, M. Chapter 2 - Semiconductor/graphene nanocomposites: Synthesis, characterization, and applications. In *Applications of Nanomaterials* (eds Mohan Bhagyaraj, S. *et al.*) 23–43 (Woodhead Publishing, 2018).

47. Hidayah, N. M. S. *et al.* Comparison on graphite, graphene oxide and reduced graphene oxide: Synthesis and characterization. *AIP Conf. Proc.* **1892**, 150002 (2017).

48. Aliyari, E., Alvand, M. & Shemirani, F. Modified surface-active ionic liquid-coated magnetic graphene oxide as a new magnetic solid phase extraction sorbent for preconcentration of trace nickel. *RSC Adv.* **6**, 64193–64202 (2016).

49. Singh, P. *et al.* Self-assembly of aromatic α-amino acids into amyloid inspired nano/micro scaled architects. *Mater. Sci. Eng. C.* **72**, 590–600 (2017).

50. Muthuselvi, C., Arunkumar, A. & Rajaperumal, G. Growth and characterization of oxalic acid doped with tryptophan crystal for antimicrobial activity. *Der Chim. Sin.* **7**, 55–62 (2016).

51. Silva, S. C. M., Fuzatto, R. H. S., Botrel, D. A., Ugucioni, J. C. & Oliveira, J. E. Development of zein nanofibers for the controlled delivery of essential amino acids for fish nutrition. *SN Appl. Sci.* **2**, 1783 (2020).

52. You, F. *et al.* Interfacial engineering of polypropylene/graphene nanocomposites: Improvement of graphene dispersion by using tryptophan as a stabilizer. *RSC Adv.* **4**, 8799–8807 (2014).

53. Liu, Z. & Li, C. Solvent-free crystallizations of amino acids: The effects of the hydrophilicity/hydrophobicity of side-chains. *Biophys. Chem.* **138**, 115–119 (2008).

54. Cullity, B. D. *Elements of X-ray diffraction* (Addison-Wesley Publishing Company, UK, 1978).

55. Li, Q., Li, F., Shen, W., Liu, X. & Cui, H. Lucigenin/Co(tryptophan)$_2$ complex bifunctionalized graphene oxide: Facile synthesis and unique chemiluminescence. *J. Mater. Chem. C* **4**, 3477–3484 (2016).

56. Nguyen, N. M. *et al.* Investigation of origin optical properties of TiO$_2$/graphene nanohybrids. *Mater. Lett.* **276**, 128042 (2020).

57. Yang, D. *et al.* Chemical analysis of graphene oxide films after heat and chemical treatments by X-ray photoelectron and Micro-Raman spectroscopy. *Carbon* **47**, 145–152 (2009).

58. Wu, J.-B., Lin, M.-L., Cong, X., Liu, H.-N. & Tan, P.-H. Raman spectroscopy of graphene-based materials and its applications in related devices. *Chem. Soc. Rev.* **47**, 1822–1873 (2018).

59. Asamoto, D. K. & Kim, J. E. UV resonance raman spectroscopy as a tool to probe membrane protein structure and dynamics. *Methods Mol. Biol.* **2019**, 327–349 (2003).

60. Tohamy, H.-A.S., El-Sakhawy, M. & Kamel, S. Development of magnetite/graphene oxide hydrogels from agricultural wastes for water treatment. *J. Renew. Mater.* **10**, 1889 (2022).

61. Maleki, B., Nasiri, N., Tayebee, R., Khojastehnezhad, A. & Akhlaghi, H. A. Green synthesis of tetrahydrobenzo[b]pyrans, pyrano[2,3-c]pyrazoles and spiro[indoline-3,4′-pyrano[2,3-c]pyrazoles catalyzed by nano-structured diphosphate in water. *RSC Adv.* **6**, 79128–79134 (2016).

62. Amoozadeh, A., Hosseininya, S. F. & Rahmani, S. Nano titania-supported sulfonic acid (n-TSA) as an efficient, inexpensive, and reusable catalyst for one-pot synthesis of 1, 8-dioxo-octahydroxanthene and tetrahydrobenzo[b]pyran derivatives. *Chem. Intermed.* **44**, 991–1011 (2018).

63. Mozafari, R. & Heidarizadeh, F. Phosphotungstic acid supported on SiO$_2$@NHPhNH$_2$ functionalized nanoparticles of MnFe$_2$O$_4$ as a recyclable catalyst for the preparation of tetrahydrobenzo[b]pyran and indazolo[2,1-b]phthalazine-triones. *Polyhedron* **162**, 263–276 (2019).

64. Maleki, B. Green synthesis of bis-coumarin and dihydropyrano[3,2-c]chromene derivatives catalyzed by o-benzenedisulfonimide. *Org. Prep. Proced. Int.* **48**, 303–318 (2016).

65. Daneshvar, N., Goli-Jolodar, O., Karimi-Chayjani, R., Nikoo Langarudi, M. S. & Shirini, F. Sustainable and Eco-friendly method for the synthesis of some bioactive derivatives of biscoumarin and Pyrano[3,2-c]Chromene-3-carbonitrile using taurine, as the catalyst. *ChemistrySelect* **4**, 1562–1566 (2019).

66. Saneinezhad, S., Mohammadi, L., Zadsirjan, V., Bamoharram, F. F. & Heravi, M. M. Silver nanoparticles-decorated Preyssler functionalized cellulose biocomposite as a novel and efficient catalyst for the synthesis of 2-amino-4H-pyrans and spirochromenes. *Sci. Rep.* **10**, 14540 (2020).

67. Amirnejat, S., Nosrati, A., Peymanfar, R. & Javanshir, S. Synthesis and antibacterial study of 2-amino-4H-pyrans and pyrans annulated heterocycles catalyzed by sulfated polysaccharide-coated BaFe$_{12}$O$_{19}$ nanoparticles. *Chem. Intermed.* **46**, 3683–3701 (2020).

68. Khazaee, A., Jahanshahi, R., Sobhani, S., Skibsted, J. & Sansano, J. M. Immobilized piperazine on the surface of graphene oxide as a heterogeneous bifunctional acid–base catalyst for the multicomponent synthesis of 2-amino-3-cyano-4H-chromenes. *Green Chem.* **22**, 4604–4616 (2020).

69. Pourian, E., Javanshir, S., Dolatkhah, Z., Molaei, S. & Maleki, A. Ultrasonic-assisted preparation, characterization, and use of novel biocompatible core/shell Fe$_3$O$_4$@ GA@ isinglass in the synthesis of 1, 4-dihydropyridine and 4 H-pyran derivatives. *ACS Omega* **3**, 5012–5020 (2018).

70. Rostami, N., Dekamin, M. G., Valiey, E. & Fanimoghadam, H. Chitosan-EDTA-Cellulose network as a green, recyclable and multifunctional biopolymeric organocatalyst for the one-pot synthesis of 2-amino-4 H-pyran derivatives. *Sci. Rep.* **12**, 8642 (2022).

71. Raji Reddy, C. & Damoder Reddy, M. A metal-free tandem C–C/C–O bond formation approach to diversely functionalized tetrasubstituted furans. *J. Org. Chem.* **79**, 106–116 (2014).

72. Keshavarz, M., Zarei Ahmady, A., Vaccaro, L. & Kardani, M. Non-covalent supported of l-proline on graphene oxide/Fe$_3$O$_4$ nanocomposite: A novel, highly efficient and superparamagnetically separable catalyst for the synthesis of bis-pyrazole derivatives. *Molecules* **23**, 330 (2018).

73. Aghaei-Hashjin, M., Yahyazadeh, A. & Abbaspour-Gilandeh, E. Zr@ IL-Fe$_3$O$_4$ MNPs as an efficient and green heterogeneous magnetic nanocatalyst for the one-pot three-component synthesis of highly substituted pyran derivatives under solvent-free conditions. *RSC Adv.* **11**, 23491–23505 (2021).

74. Hummers, W. S. & Offeman, R. E. Preparation of graphitic oxide. *J. Am. Chem. Soc.* **80**, 1339–1439 (1958).

Author contributions
L.A.Z. done the experimental section and analyzed the results. S.K. wrote the main manuscript text. All authors reviewed the manuscript. We confirm that the manuscript has been read and approved by all named authors and the order of authors listed in the manuscript has been approved by all of us.

Competing interests
The authors declare no competing interests.

Additional information
Supplementary Information The online version contains supplementary material available at https://doi.org/10.1038/s41598-024-57682-y.

Correspondence and requests for materials should be addressed to S.K.

Reprints and permissions information is available at www.nature.com/reprints.

Publisher's note Springer Nature remains neutral with regard to jurisdictional claims in published maps and institutional affiliations.